ISSN 0036-0295, Russian Metallurgy (Metally), Vol. 2017, No. 13, pp. 1194–1201. © Pleiades Publishing, Ltd., 2017.
Original Russian Text © S.I. Koshoridze, Yu.K. Levin, L.N. Rabinskiy, A.V. Babaytsev, 2016, published in Tekhnologiya Metallov, 2016, No. 12, pp. 24–33.

EQUIPMENT AND DEVICES

Investigation of Deposits in Channels of Panels of a Heat-Transfer Agent

S. I. Koshoridze[a], Yu. K. Levin[a], L. N. Rabinskiy[b, *], and A. V. Babaytsev[b]

[a] *Institute of Applied Mechanics, Russian Academy of Sciences, Moscow, Russia*
[b] *Moscow Institute of Aviation, Moscow, Russia*
**e-mail: Ar7eny-f_i@mail.ru*

Received June 5, 2016

Abstract—An analysis of the behavior of nanosized colloidal particles in a supersaturated solution made it possible to substantiate the possibility of increasing the heat-transfer efficiency in a heat exchanger during magnetic treatment of a heat-transfer agent. A model is proposed to weaken the scale during magnetic treatment of a water stream. A colloidal solution is shown to decrease its stability—the coagulation of colloidal particles begins—because of the deformation of the double electrical layer. As a result of increasing the effective radius of curvature of nanoparticles, the solution becomes strongly supersaturated with respect to forming aggregates, which accelerates the solidification of dissolved salts on them. The influence of the interfacial layer of nanoobjects decreases the energy of formation of critical nuclei (size effect) and their sizes. Since coagulation tends to decrease the concentration of critical nuclei in the solution, their loss should be compensated via the homogeneous generation of new nuclei. As a result, the concentration of suspended particles increases additionally and the antiscale effect is enhanced. The solidification flux of dissolved salts is shown to deposit mainly on suspended nanoparticles due to an increase in their total surface area and to the fact that the coefficient of mass transfer to suspension is higher than that to the wall by four orders of magnitude. The mathematical model constructed on the basis of the detected set of physical processes can be used to perform quantitative estimates of the antiscale effect in real power plants.

Keywords: nanoparticle, salt, coagulation, scale, colloidal particle, supersaturated solution, nucleus, magnetic treatment, heat-transfer agent

DOI: 10.1134/S0036029517130092

INTRODUCTION

The increase in the heat exchanger efficiency is substantially related to a decrease in the scale on heat-exchange panels. One of the technologies intended to solve this problem is magnetic treatment of a water stream to decrease the scale.

Scale formation is known to be a serious problem in heat power engineering, since every scale millimeter on the boiler wall leads to a decrease in the heating power by 5–10%, which is illustrated in Fig. 1 (data of Lifescience Company, Great Britain [1]).

To struggle against scale formation, engineers treat a water stream by a magnetic field, which is simple and efficient. However, a generally accepted theory that could explain the mechanism of this phenomenon is still absent despite the fact that the history of the problem begins with the first world patent granted for apparatus for magnetic water treatment (MWT) to Wermeiren in 1946.

However, the causes of this effect have long been unknown. Obviously, the complexity of the problem consists in the fact that the processes responsible for the effects occur on a nanoscale and the approaches required for understanding the essence of the phenomenon had not been developed, since nanomechanics methods have recently been developed. In particular, it has been recently shown that nanosized manifest themselves in the influence of an interfacial layer on the new surface formation energy, the sizes of the critical nuclei that form during homogeneous generation, and their equilibrium concentration.

The mechanism of the phenomenon was first explained in the theory of stability of lyophobic colloids, the so-called DLVO (Deryagin–Landau–Verwey–Overbeek) theory [2]. According to this theory, colloidal particles, which are neutral as a whole, carry electric charges and are surrounded by a double electrical layer (DEL). In the left-hand side in Fig. 2, the central core of a colloidal particle with positive potential-forming ions is surrounded by a dense layer of negative counterion charges, which is called the Stern layer. A relatively wide layer of counterions, i.e., a diffusion layer, is located behind the Stern layer around the colloidal particle. These counterions are not sorbed on the Stern layer, since thermal motion energy

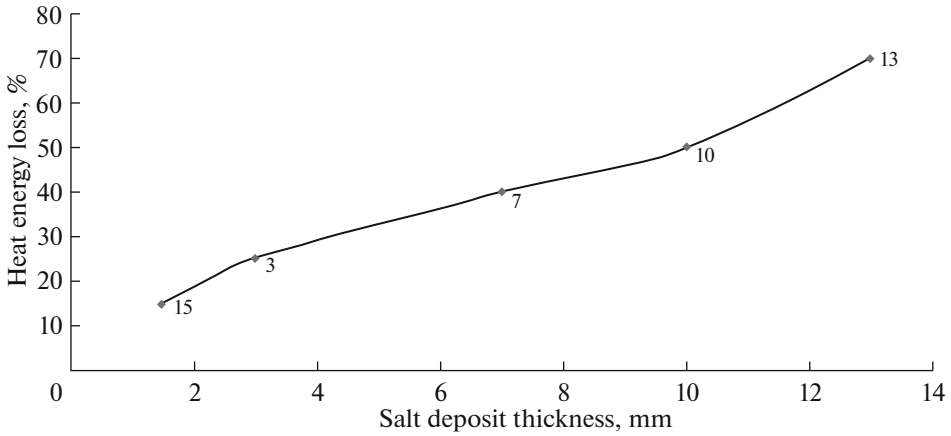

Fig. 1. Heat energy loss for heat transfer through a heating surface.

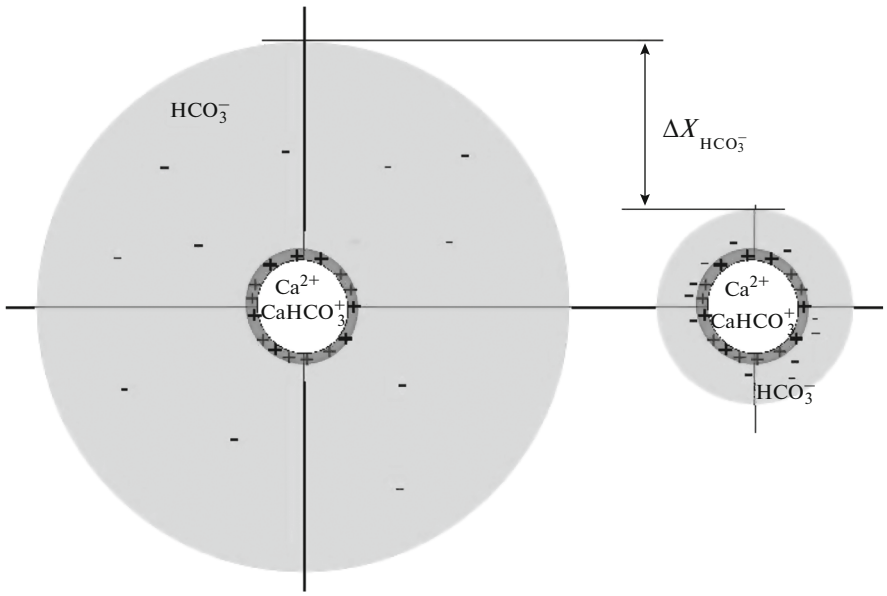

Fig. 2. Decrease in the DEL thickness of a colloidal particle in a magnetic field.

kT and the water dipole molecules surrounding the core of the particle do not disturb them.

Colloidal particles in a solution interact with each other, and the Coulomb repulsion forces of the charges in the diffusion layer are compensated by the molecular attraction forces, which ensures stability of a colloidal solution according to the DLVO theory.

Gamayunov [4] explained the possibility of the influence of a magnetic field on the physicochemical processes that occur in the water stream intersecting it. He showed that the DEL thickness decreases by ΔX due to the Lorentz forces when a DEL-surrounded particle moves in a transverse magnetic field (with allowance for its rotation; see the right-hand side of Fig. 2).

As a result of magnetic treatment, the electrokinetic potential of colloidal particles decreases, the potential barrier of their repulsion from each other lowers substantially, and the probability of their coagulation increases.

Thus, the first specific feature of the chain of significant effects during MWT consists in the fact that a magnetic field deforms the DEL of colloidal particles and initiates their coagulation in a supersaturated water solution.

CHANGE IN THE SOLUTION AFTER ITS MAGNETIZATION

When considering the initial state of a colloidal solution, we note that critical nuclei do not grow due

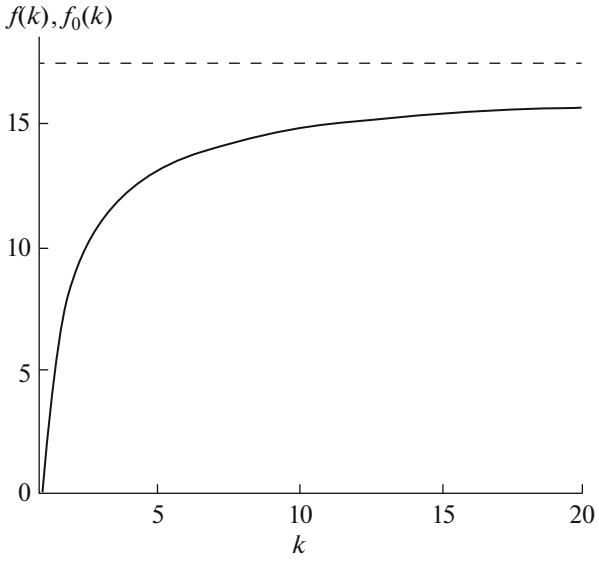

Fig. 3. Relative supersaturation $f(k)$ vs. coagulation stage number k (solid line). Supersaturation of solution f_0 = 17.57 (dashed straight line).

to the solidification of scale salts on them, since the solution is not supersaturated with respect to such small particles by definition and the probabilities of sorption and desorption of salt molecules on them are the same. After magnetization of the solution, nuclei grow as a result of coagulation and acquire supercritical sizes. We can show that the kth particle (it forms in the kth stage of coagulation and consists of k critical nuclei) has radius $\sqrt[3]{k}r_{cr}$, the equilibrium concentration of scale-forming molecules in water C_k corresponds to it, and the relation [4]

$$f(k) = \frac{C}{C_0} - \left(\frac{C}{C_0}\right)^{\frac{1}{\sqrt[3]{k}}} \quad (1)$$

is valid for relative supersaturation $f(k) = (C - C_k)/C_0$.

Figure 3 (solid line) shows relative supersaturation $f(k)$ versus coagulation stage number k.

The supersaturation for a flat interface $f_0 = (C - C_k)/C_0$ = 17.57 at a solution concentration C = 2.6 mol/m^3 and its equilibrium value C_0 = 14 mol/m^3 for a flat interface is shown by the dashed line in Fig. 3. This curve demonstrates that the initial relative solution supersaturation ($f(1) = 0$ for critical nuclei) with respect to the nucleus of double mass increases sharply to $f(2) = (C - C_2)/C_0 = 8.4$ upon the first collision of critical nuclei ($k = 2$) in a magnetized water stream, and this supersaturation increases to $f(3) = 11$ for the next collision.

This behavior causes intense solidification of dissolved scale salts in the magnetized water stream volume and prevents the deposition of salts on the tube walls. Thus, the second specific feature of the behavior of a magnetized water stream consists in the fact that the supersaturation of the solution with respect to suspension increases sharply at the initial stage of coagulation. As a result, its concentration in the water stream increases, which makes a contribution to the antiscale effect.

ANALYSIS OF THE COAGULATION OF COLLOIDAL PARTICLES IN A MAGNETIZED WATER STREAM

We now describe the coagulation intensity to obtain quantitative estimates. Assume that colloidal particles of a critical radius with equilibrium concentration n_0 are present in a solution with a given supersaturation and that the system is in dynamic equilibrium. To calculate the time evolution of the concentration of primary, secondary, etc., colloidal particles $n_k(t)$, we use the expression [5]

$$n_k(t) = n_0\left(\frac{t}{\tau_0 + t)}\right)^{k-1}, \quad k = 1, 2, 3, \ldots, \quad (2)$$

where τ_0 is the so-called coagulation time [2], n_0 is the initial concentration of particles, and $n_1(t) = n_0$ = const is the relation that refines the Smoluchowski formula [2].

The necessity of refinement is caused by the following behavior of a supersaturated solution [6]: when considering the phase transition kinetics, the authors of [6] postulated that a solution under stable thermodynamic conditions should maintain the equilibrium concentration of critical nuclei. The decrease in their number during coagulation should be accompanied by an increase in their concentration to an equilibrium value due to homogeneous nucleation of new particles in the volume of a supersaturated solution, which was not taken into account in the Smoluchowski theory of fast coagulation. This correction is substantial, since the appearance of new nuclei increases the suspension surface and also contributes to the antiscale effect.

Thus, the third specific feature of the behavior of a magnetized water stream consists in the fact that, during the coagulation of colloidal particles of a critical size, homogeneous generation of new critical nuclei appears to restore their equilibrium concentration under stable thermodynamic conditions. This specific feature increases the intensity of solidification of the salts dissolved in the water stream volume. We will show that this phenomenon is directly related to a decrease in the scale on the heat-exchange unit walls.

INFLUENCE OF THE NANOSIZE OF CRITICAL NUCLEI ON THEIR EQUILIBRIUM CONCENTRATION

We assume that the water solution of salt $CaCO_3$ only has nuclei of near-critical size r_{cr}: larger nuclei are absent because of the low probability of their for-

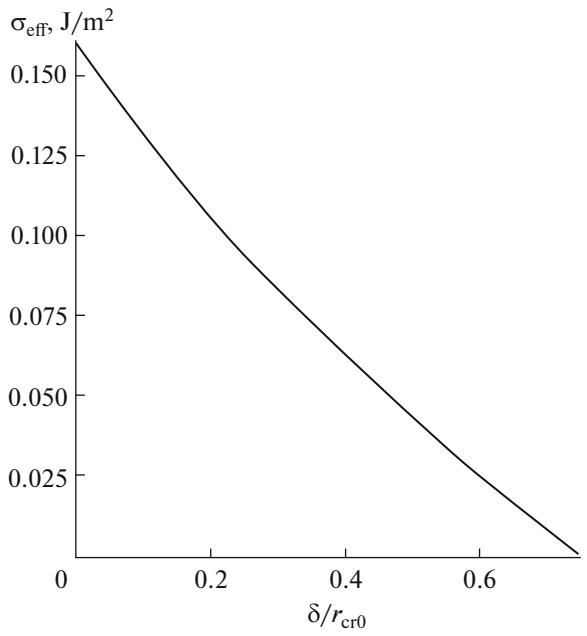

Fig. 4. Surface tension at the nucleus/water interface vs. dimensionless Tolman parameter δ/r_{cr0}.

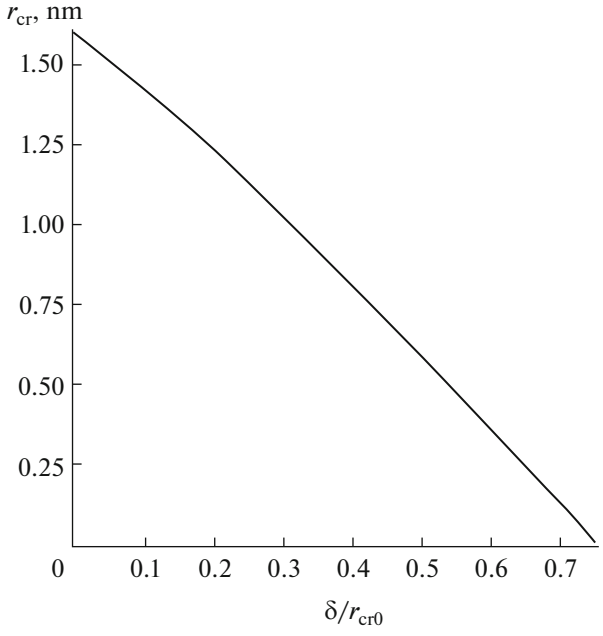

Fig. 5. Critical nucleus radius r_{cr} vs. dimensionless Tolman parameter δ/r_{cr0}.

mation, and smaller nuclei disappear right after appearance.

As was shown in [7], the mass-transfer characteristics in a supersaturated solution, where the surface radius is comparable with the interfacial region thickness, form with allowance for Tolman constant δ. As a result, we use the following expression, which takes into account the size effect, instead of nominal critical radius r_{cr0} [5]:

$$r_{cr} = \frac{r_{cr0}}{2}\left(1 - \frac{4\delta}{r_{cr0}} + \sqrt{\frac{4\delta + r_{cr0}}{r_{cr0}}}\right). \quad (3)$$

Similarly, effective surface energy σ_{eff} at the liquid/crystal interface decreases and takes the form

$$\sigma_{eff} = \frac{\sigma_{s.l}}{1 + \dfrac{2\delta}{r_{cr}}}, \quad (4)$$

where $\sigma_{s.l}$ is the surface tension at the flat solid/liquid interface and parameter δ takes values in the range $0 \geq \delta \geq 1.5r_{cr0}$. In this case, the probability of homogeneous formation of a nanosized nucleus, which is determined by effective value σ_{eff}, increases substantially.

It should be noted that the estimates given below [8] are presented for the experimental conditions from [9]. Figure 4 shows the effective surface tension at the nucleus/water interface (Eq. (4)) versus dimensionless Tolman parameter δ/r_{cr0}.

Figure 5 depicts critical nucleus radius r_{cr} (Eq. (3)) versus dimensionless Tolman parameter δ/r_{cr0}.

The number of molecules in a critical nucleus is

$$N_{cr} = \frac{\dfrac{4}{3}\pi r_{cr}^3}{\dfrac{M}{\rho N_A}}. \quad (5)$$

Allowing for Eq. (4), in Fig. 6 we plot the number of molecules in a critical nucleus N_{cr} (Eq. (5)) versus dimensionless Tolman parameter δ/r_{cr0}.

According to the thermodynamic fluctuation theory, the probability density of formation of a nucleus of size r in a supersaturated solution is proportional to factor $\exp[-\Delta G(r)/k_B T]$, where $\Delta G(r)$ is the minimum energy required for the creation of the given nucleus at a fixed temperature and pressure. This energy is equal to the change in the thermodynamic Gibbs potential [6]. With allowance for the size effect [7], the Gibbs energy of nucleus formation is calculated by the formula

$$\Delta G(r) = \frac{4\pi r^3 \sigma_{s.l}}{3}\left(\frac{3}{r + 2\delta} - \frac{2}{r_{cr0}}\right).$$

For a critical nucleus, it transforms into the expression

$$\Delta G_{cr} = \frac{4\pi r_{cr}^3 \sigma_{s.l}}{3}\left(\frac{3}{r_{cr} + 2\delta} - \frac{2}{r_{cr0}}\right). \quad (6)$$

Figure 7 shows the Gibbs energy of critical nucleus ΔG_{cr} versus dimensionless Tolman parameter δ/r_{cr0}.

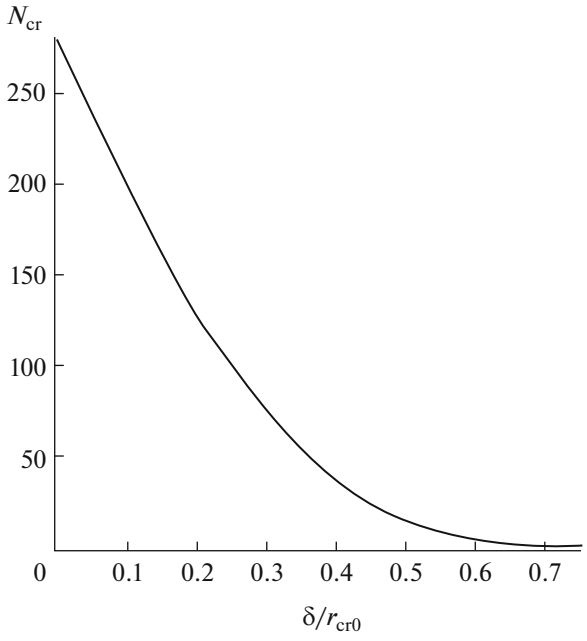

Fig. 6. Number of molecules in a critical nucleus N_{cr} vs. dimensionless Tolman parameter δ/r_{cr0}.

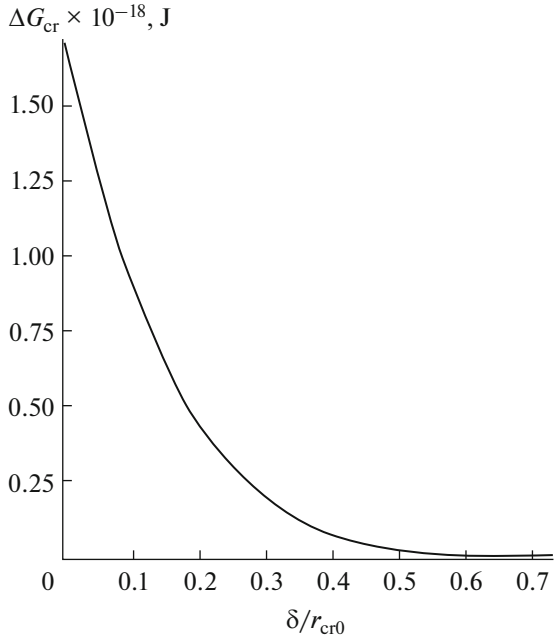

Fig. 7. Free Gibbs energy of critical nucleus formation ΔG_{cr} vs. dimensionless Tolman parameter δ/r_{cr0}.

When estimating the equilibrium concentration of suspended particles, we are interested in only the nuclei having near-critical sizes. Following [6], we expand function $\Delta G(r)$ in small parameter $r - r_{cr}$, retain quadratic terms, take into account that the first derivative is zero at a maximum by definition, and obtain

$$\Delta G(r) \approx \Delta G_{cr} + \frac{1}{2}\left.\frac{d^2\Delta G}{dr^2}\right|_{(r=r_{cr})}(r - r_{cr})^2.$$

For the distribution of nuclei with near-critical sizes, we take into account Zel'dovich factor A_z [10] and find

$$f(r) = \frac{r_{cr}^2 A_z}{V_l V_s}\exp\left(-\frac{\Delta G_{cr}}{k_B T}\right)\exp\left[\frac{b(r - r_{cr})^2}{2k_B T}\right], \quad (7)$$

where $V_l = 1/CN_A$ and $V_s = M/\rho N_A$ are the volumes per $CaCO_3$ molecule in the liquid (water) and solid (nucleus) phases, respectively, and $A_z = \left(\Delta G_{cr}\Big/3\pi k_B T N_{cr}^2\right)^{0.5}$.

b is determined by the formula

$$b = -\left.\frac{d^2\Delta G}{dr^2}\right|_{r = r_{cr}} > 0.$$

Radius r_{cr} corresponds to the critical region where the free Gibbs energy falls in the range determined by thermal fluctuation $k_B T$. Here, we have

$$r_{cr} - \delta r_{cr} \le r \le r_{cr} + \delta r_{cr}, \text{ where } \delta r_{cr} = \sqrt{\frac{k_B T}{4\pi\sigma_{eff}}},$$

where $M = 0.1$ kg/mol is the molar mass of $CaCO_3$ and $\rho = 2711$ kg/m^3 is the density of the solid $CaCO_3$ phase.

Allowing for Eq. (7), we find the equilibrium concentration of critical nuclei n_0 (m^{-3}) versus dimensionless Tolman parameter δ/r_{cr0}, $n_0 = \int_{r_{cr}-\delta_{cr}}^{r_{cr}+\delta r_{cr}} f(r)dr$.

Figure 8 depicts this dependence.

As was shown above, the fourth specific feature of the behavior of a magnetized water stream consists in the fact that the related processes have nanoscales. Therefore, their characteristics (Gibbs energy ΔG of formation of critical nuclei, their sizes r_{cr}, equilibrium concentration n_0) depend substantially on the interfacial layer characterized by the Tolman constant. According to Eq. (7), the influence of this constant on the Gibbs energy leads to an exponential increase in the intensity of homogeneous generation of critical nuclei, which increases the concentration of suspended particles in a magnetized water stream that is detected in practice [11].

DIFFERENCE BETWEEN THE PROCESSES OF MASS TRANSFER TO THE WALL AND THE SUSPENSION

Dissolved salts deposit onto the solid surfaces of both suspended particles and the tube walls and form a scale to be struggled with.

As was shown in [8], the processes of mass transfer to the heat exchanger wall and the surface of sus-

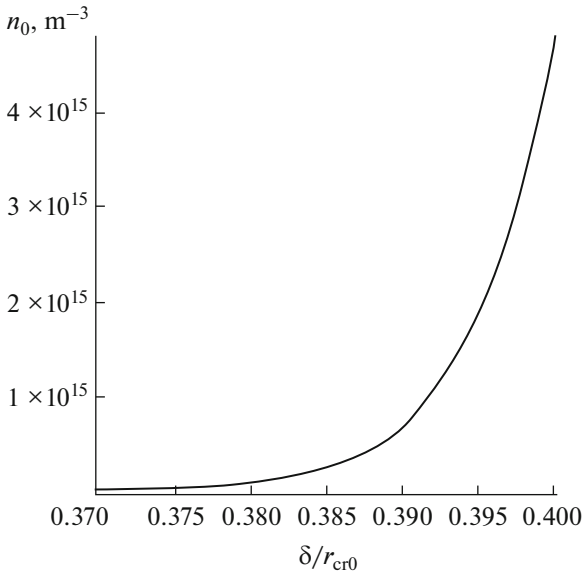

Fig. 8. Equilibrium concentration of critical nuclei n_0 vs. dimensionless Tolman parameter δ/r_{cr0}.

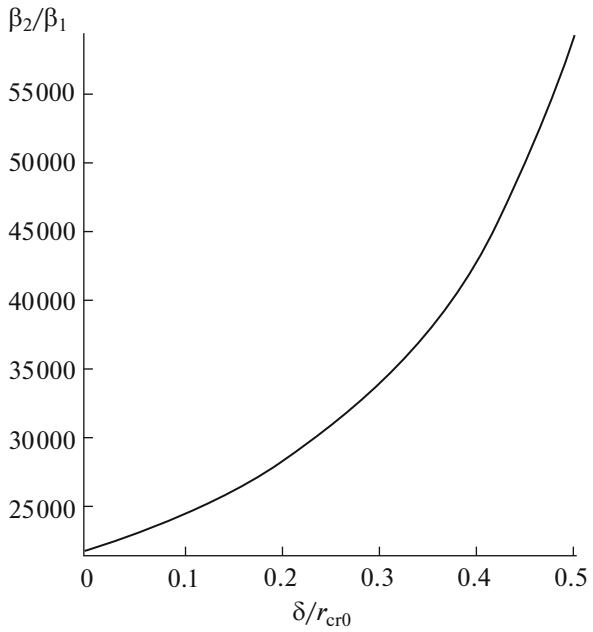

Fig. 9. Ratio of the coefficients of mass transfer to the suspension and the walls β_2/β_1 vs. dimensionless Tolman parameter δ/r_{cr0}.

pended crystals are radically different and obey different laws. The former process depends on the hydrodynamics of the turbulent flow in a round tube of diameter d, is characterized by mass-transfer coefficient β_1 (m/s), and is determined by the formula [12]

$$\beta_1 = 0.023\,\mathrm{Re}^{-0.2}\,\mathrm{Pr}^{-2/3}\,u, \qquad \mathrm{Re} = \frac{ud}{\nu},\ \ \mathrm{Pr} = \frac{\nu}{D}, \tag{8}$$

where Re and Pr are the Reynolds number and the Prandtl number, respectively; u is the water stream speed in the tube; ν is the kinematic viscosity of water; and D is the diffusion coefficient of molecules in water.

The second process is determined by the mass transfer to a solid sphere in an immobile medium, since suspended particles (critical nuclei) are trapped along with a liquid stream. Here, mass-transfer coefficient β_2 is [13]

$$\beta_2 = \frac{D}{r_{cr}}. \tag{9}$$

Using Eqs. (8)–(9) and the conditions from [9] ($\nu = 10^{-6}$ m^2/s at temperature $T = 300$ K, $d = 0.03$ m, $D = 10^{-9}$ m^2/s, $u = 0.5$ m/s), we determine the dependence of the ratio of the coefficients of mass transfer to the suspension and the walls on the dimensionless Tolman parameter. Figure 9 shows this dependence, from whence it is seen that $\beta_2/\beta_1 > 10^4$.

Thus, the fifth physical factor that affects the efficiency of the antiscale activity of a magnetic field is a higher rate of mass transfer of dissolved salts to the suspension due to molecular diffusion in comparison with their mass transfer to the tube walls from a turbulent flow.

This effect is additionally enhanced by the influence of the interfacial region thickness (Tolman constant δ) on the energy characteristics of nuclei in a supersaturated water stream, which was noted above.

THEORETICAL ESTIMATION OF THE ANTISCALE EFFECT

When revealing the specific features of a water stream subjected to magnetic treatment, we pass to estimating the result, namely, the reducing of scale. Here, we take into account that the concentration of dissolved salts in the experiment in [9] remained almost unchanged at a 30-fold decrease in the scale on the walls after water magnetization. Therefore, the hypothesis that the total flux of solidified salts from a supersaturated solution does not change after magnetization holds true: solidification simply switches from the walls to the suspension. In other words, the flux of scale-forming molecules to the walls before MWT is equal to the flux to the suspension and the walls after MWT. Hence, the coefficient of reducing the scale on the heat exchanger walls Θ due to MWT is

$$\Theta = 1 + \frac{\sum_{k=2} I_{2k\mathrm{mag}}}{\beta_{1,\mathrm{mag}} L\pi d(C - C_0)}. \tag{10}$$

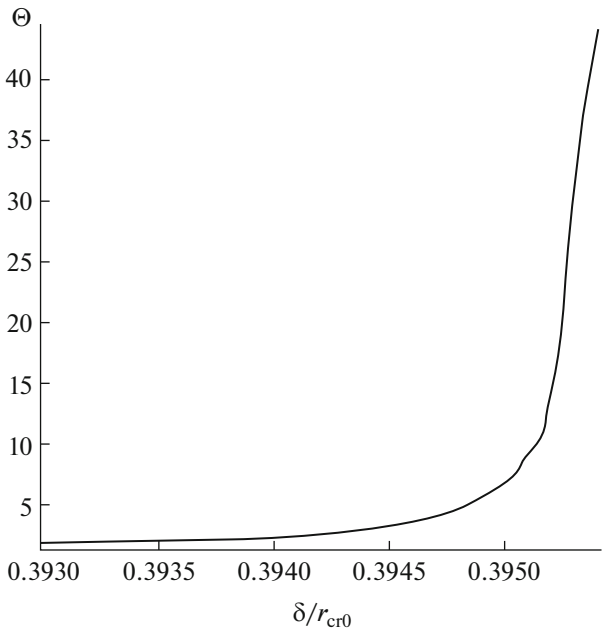

Fig. 10. Antiscale effect Θ vs. normalized Tolman constant.

Here, the solidification flux of $CaCO_3$ molecules $I_{2k\text{mag}}$ (mol/s) to the total surface of colloidal particles of the kth ($k = 2, 3, ...$) order in a magnetized solution is

$$I_{2,\text{mag}}(k) = \beta_2(k)\frac{\pi d^2}{4} \times 4\pi r_{\text{cr}}^2 \times \sqrt[3]{k^2}\left(C - C_0\left(\frac{C}{C_0}\right)^{\frac{1}{\sqrt[3]{k}}}\right)\int_0^L n_k(x)dx, \quad (11)$$

where πLd is the surface are of a tube of diameter d and length L (when deriving this formula, we neglected the changes in the sizes of colloidal particles during motion along the tube), $\beta_{1\text{mag}}$ is the coefficient of mass transfer to the heat exchanger wall surface during MWT, $\beta_2(k)$ is the coefficient of mass transfer to suspended particles of the kth order (m/s), $n_k(x)$ is the concentration of colloidal particles of the kth order at distance x from the beginning of the tube (m^{-3}), and C_0 is the equilibrium molar concentration of $CaCO_3$ molecules in water (mol/m^3) at which the probabilities of their sorption and desorption onto the flat solid/liquid interface are the same.

In Eq. (11), we took into account the change in the supersaturation of the solution (Eq. (1)) during coagulation.

Note that Eq. (10) is not final, since its right-hand side contains $\beta_{1\text{mag}}$, which depends on Θ. Indeed, by definition, the decrease in the scale is determined by the expression

$$\Theta = \frac{\beta_1 L\pi d(C - C_0)}{\beta_{1,\text{mag}} L\pi d(C - C_0)} = \frac{\beta_1}{\beta_{1,\text{mag}}}, \quad (12)$$

from whence we have

$$\beta_{1,\text{mag}} = \frac{\beta_1}{\Theta}.$$

The substitution of $\beta_{1\text{mag}}$ leads to the formula

$$\Theta = \frac{\beta_1 L\pi d(C - C_0)}{\beta_1 L\pi d(C - C_0) - \sum_{k=2}\beta_2(k)S_k(C - C_k)}. \quad (13)$$

Figure 10 shows the results of calculating antiscale effect Θ as a function of the ratio δ/r_{cr0}. When plotting this dependence, we calculated the radius of the critical nucleus r_{cr} and nucleus concentration n at every value of δ and then calculated antiscale effect Θ.

Summarizing the aforesaid, we note that the sixth physical factor in the mechanism of magnetic treatment consists in the fact that, when the concentration of suspended particles in the water volume increases, solidification switches to suspension due to both an increase in the suspension concentration and a high coefficient of mass transfer to it.

CONCLUSIONS

To determine the possibility of increasing the efficiency of heat transfer in heat exchangers due to a weakening of the scale, we considered the behavior of a supersaturated solution of $CaCO_3$ salts during magnetic treatment of a heat-transfer agent. We used Gamayunov's hypothesis, according to which the action of a magnetic field leads to the loss of stability of a colloidal solution because of the deformation of DEL and critical nuclei in it begin to coagulate. We then took into account that particles with a radius larger than the critical radius appear in the solution and scale molecules from the supersaturated solution deposit onto them via heterogeneous solidification. The following six factors were shown to determine the antiscale effect.

(1) The deformation of DEL initiates the coagulation of colloidal particles.

(2) At the initial stages of coagulation, the supersaturation of the solution increases sharply with respect to coagulated particles.

(3) The mass transfer of solidifying molecules from the water solution to nanosized suspension is much more active than that to the heat exchanger walls.

(4) The specific energy of new surface formation decreases substantially for nanosized critical nuclei, which exponentially increases the rate of their homogeneous generation and their concentration in the solution.

(5) A decrease in the concentration of critical nuclei is continuously compensated due to the homogeneous generation of new critical nuclei in order to retain dynamic equilibrium between the liquid and solid phases in the supersaturated solution.

(6) An increase in the suspension concentration in the volume of a magnetized water stream leads to a radical redistribution of scale between the wall and the suspension toward the latter, which determines the detected antiscale effect of magnetic treatment.

Thus, we can conclude that this set of well-known physical phenomena results in an antiscale effect ($\Theta = 30$), as in the experiment in [9], and the Tolman constant at which this effect takes place agrees with the well-known estimate of its range [7]. On the whole, this finding supports the hypothesis [14–17] regarding the mechanism of reducing the scale during MWT.

Note, in conclusion, that we were able to clarify the problem of magnetic treatment of a water stream, which was unclear since the first half of the last century, only using nanomechanics tools and the laws that are characteristic of nanosized objects.

ACKNOWLEDGMENTS

Financial support from Russian Federal Targeted Program "Research and Development under Priority Areas of Russian Science and Technology on 2014-2020 years," Agreement No. 14.574.21.0166 (identifier RFMEFI57417X0166).

REFERENCES

1. http://elektrokotly.ru.
2. *Colloid Science. Vol. 1. Irreversible Systems*, Ed. by H. R. Kruyt (Elsevier, Amsterdam, 1952).
3. N. Y. Gamayunov, "Action of a static magnetic field on moving solutions and suspensions," Colloid Journal **56** (2), 234–241 (1994).
4. S. I. Koshoridze and Yu. K. Levin, "The influence of colloid particle coagulation on the reduction of scale formation during magnetic treatment of water in thermal power devices," Thermal Engineering **58**, 547–551 (2011).
5. S. I. Koshoridze and Yu. K. Levin, "The mechanism of reducing scale during magnetic water treatment in heat-power devices," Thermal Engineering **60** (3), 227–230 (2013).
6. E. M. Lifshitz and L. P. Pitaevski, *Physical Kinetics: Course of Theoretical Physics* (Pergamon Press, New York, 1981), Vol. 10.
7. A. F. Puzryakov, I. N. Kravchenko, A. A. Kolomeichenko, M. Yu. Putyrskaya, A. S. Osipkov, and A. A. Puzryakov, "New apporaches to increasing the resource of mechanical parts by gas thermal sputtering of nanostructured materials," Remont, Vosstanovlenie, Modernizatsiya, No. 6, 32–35 (2014).
8. I. N. Kravchenko, A. F. Puzryakov, A. A. Puzryakov, A. A. Kolomeichenko, and I. Yu. Lobov, "On the problem of the effect of the design-technological parameters on the strength of a deposited coating," Remont, Vosstanovlenie, Modernizatsiya, No. 11, 40–42 (2015).
9. A. Szkatula, M. Balanda, and M. Kopec, "Magnetic treatment of industrial water. Silica activation," The Europ. Phys. J. Appl. Phys. **18**, 41–49 (2002).
10. I. A. Sluchinskaya, *Fundamentals of the Materials Science and Technology of Semiconductors* (Izd. NIFI, Moscow, 2002).
11. V. I. Klasen, *Magnetization of Water Systems* (Khimiya, Moscow, 1982).
12. J. S. Newman, *Electro-Chemical Systems* (University of California, California, 1973).
13. T. K. Sherwood, R. L. Picford, and C. R. Wilke, *Mass Transfer* (McGraw-Hill, New York, 1975).
14. S. I. Koshoridze and Yu. K. Levin, "The influence of a magnetic field on the coagulation of nanosized colloid particles," Technical Physics Letters **40** (8), 736–739 (2014).
15. Yu. K. Levin, "Generation of aragonite nanocrystals in a magnetized water flow," Nanomechanics Science and Technology **5** (1), 23–31 (2014).
16. S. I. Koshoridze and Yu. K. Levin, "Determining the range of dimensions of nanomechanics objects," Nanomechanics Science and Technology **5** (2), 141–151 (2014).
17. S. I. Koshoridze and Yu. K. Levin, "Z-potential of colloidal nanoparticles as a function of magnetic treatment time and temperature," Nanomechanics Science and Technology **5** (3), 169–179 (2014).

Translated by K. Shakhlevich